RESEARCH PAPER

Comparative evaluation of cytotoxicity and inflammatory responses induced by free and eugenol-loaded titanium dioxide nanoparticles following intraperitoneal injection in mouse

Farazdaq Nazar Al-Naffakh[1], Somayeh Reiisi[1*], Norolhoda Khalighi[2], Elham Moghtadaei Khorasgani[3]

[1] Department of Genetics, Faculty of Basic Sciences, Shahrekord University, Shahrekord, Iran
[2] Department of Pathobiology, Faculty of Veterinary Medicine, Shahrekord University, Shahrekord, Iran
[3] Department of Pathobiology, Shahrekord Branch, Islamic Azad University, Shahrekord, Iran

ABSTRACT

Objective(s)*:* Titanium dioxide nanoparticles (TiO_2 NPs), which are widely used in food and consumer products, have been associated with oxidative stress and inflammatory toxicity. Eugenol, a naturally occurring phenolic compound with well-established anti-inflammatory and antioxidant properties, may exert protective effects when delivered through nanocarriers.

Materials and Methods*:* TiO_2 nanoparticles were synthesized via a co-precipitation method and subsequently functionalized with eugenol (TiO_2@eugenol). FTIR, XRD, DLS, zeta potential analysis, FE-SEM, and TEM were used to characterize the nanoparticles. Thirty-six BALB/cJ mice were randomly assigned to six groups (n = 6 per group). They received intraperitoneal injections of free eugenol, TiO_2 nanoparticles, or TiO_2@eugenol at low (50 mg/kg) or high (200 mg/kg) doses for 14 days. Following the treatment period, serum concentrations of IL-1β, IL-6, and TNF-α were measured using ELISA; hepatic caspase-3/7 activity was assessed; and histological examinations of the liver, kidney, and spleen were performed. Gene expression of antioxidant markers (SOD3, GR, GPx) in liver tissue was evaluated by qRT-PCR.

Results*:* TiO_2 NPs significantly increased pro-inflammatory cytokines and hepatic caspase-3/7 activity. They also induced necrosis and inflammatory alterations in the liver, kidney, and spleen. In contrast, TiO_2@eugenol markedly suppressed cytokine release and apoptotic activity while preserving tissue architecture. qRT-PCR analysis showed that TiO_2 NPs downregulated antioxidant-related genes, whereas TiO_2@eugenol significantly upregulated their expression, indicating improved redox homeostasis.

Conclusion*:* Eugenol functionalization improved the biocompatibility profile of TiO_2 NPs and provided substantial protection against TiO_2-induced toxicity by attenuating inflammation, apoptosis, and oxidative stress while restoring antioxidant defenses. These findings highlight the therapeutic potential of eugenol-loaded TiO_2 nanoparticles and support further investigation in extended exposure models and disease-specific applications.

Keywords: *Titanium dioxide; NPs; Eugenol; Inflammation; Cytotoxicity*.

How to cite this article

Al-Naffakh FN, Reiisi S, Khalighi N, Moghtadaei Khorasgani E. Comparative evaluation of cytotoxicity and inflammatory responses induced by free and eugenol-loaded titanium dioxide nps following intraperitoneal injection in mouse. Nanomed J. 2026; 13(2): 356-370. DOI: 10.22038/NMJ.2025.90454.2286

INTRODUCTION

The advent of nanotechnology has revolutionized multiple scientific disciplines by enabling the design, modification, and application of materials at the nanoscale. At this dimension, materials exhibit unique physicochemical properties that differ substantially from those of their bulk counterparts, including enhanced reactivity, improved solubility, and altered biological interactions [1, 2]. Among the wide range of engineered nanomaterials, titanium dioxide nanoparticles (TiO_2 NPs) have attracted considerable attention due to their biocompatibility, stability, photocatalytic activity,

* *Corresponding author:* Somayeh Reiisi; PhD, Department of Genetics, Faculty of Basic Sciences, Shahrekord University, Shahrekord, Iran. Email address: s.reiisi@yahoo.com; s.reiisi@sku.ac.ir.

Note. This manuscript was submitted on August 14, 2025; approved on November 26, 2025.

and cost-effectiveness. These nanoparticles are widely incorporated into cosmetics, sunscreens, paints, and food additives owing to their UV-blocking and whitening capabilities [3-5]. Furthermore, their emerging biomedical applications—such as antimicrobial therapies and targeted drug delivery—have intensified research into their interactions with biological systems. Despite these advantages, growing evidence indicates that TiO_2 NPs may elicit unintended cytotoxic and immunotoxic responses, particularly following systemic exposure [6, 7].

Nanoparticles such as TiO_2 can interact with biological fluids and tissues, forming a protein-rich coating known as the bio-corona. This layer, composed of proteins, lipids, and other biomolecules, defines the nanoparticle's biological identity and influences its cellular uptake, biodistribution, and immunogenicity [8, 9]. Upon internalization—particularly by immune cells such as macrophages and dendritic cells—TiO_2 NPs may initiate inflammatory signaling through mechanisms involving oxidative stress, inflammasome activation, and cytokine release [10, 11]. Prolonged exposure or accumulation of these particles may consequently result in chronic inflammation, tissue injury, or, in some cases, tumorigenesis [12, 13]. A major pathway through which nanoparticles exert toxicity is the excessive generation of reactive oxygen species (ROS). This occurs when the surface of TiO_2 NPs catalyzes redox reactions under UV or visible light exposure. ROS overproduction can induce oxidative damage to proteins, lipids, and nucleic acids, ultimately impairing cellular function and initiating apoptosis or necrosis [14, 15]. The anatase crystalline form of TiO_2 is particularly noted for its heightened photocatalytic activity and ROS-generating capacity, making it more bio-reactive—and potentially more toxic—than the rutile form [16, 17]. In light of these toxicological concerns, naturally derived compounds with antioxidant and anti-inflammatory properties have been explored as potential modifiers to mitigate NP-induced damage. One such compound is eugenol, a phenolic phytochemical predominantly found in clove, cinnamon, tulsi, and other aromatic plants. It exhibits a broad spectrum of biological activities, including antimicrobial, antioxidant, anti-inflammatory, and anticancer effects [18-20]. These properties position eugenol as a promising candidate for functionalizing or loading onto nanoparticles to enhance their therapeutic utility while diminishing toxicity. Recent research suggests that eugenol can attenuate inflammatory responses by reducing cytokine production, scavenging ROS, and stabilizing cellular membranes [20, 21]. When incorporated into nanoparticles, eugenol not only enhances biocompatibility but may also modulate immune function by lowering macrophage activation and neutrophil recruitment. Thus, eugenol-loaded TiO_2 NPs represent an innovative approach that integrates the structural advantages of nanomaterials with the biological potency of phytochemicals. Furthermore, the immune response to TiO_2 NPs is highly dependent on the nanoparticle's size, morphology, surface charge, and surface functionalization. These characteristics determine how the immune system recognizes and interacts with the particle, influencing processes such as opsonization, phagocytosis, and cytokine production [10, 22]. In the absence of surface modification, TiO_2 NPs are often perceived as foreign entities, triggering innate immune responses via toll-like receptors (TLRs) and inflammasome pathways, such as NLRP3. These interactions promote the release of pro-inflammatory cytokines, including IL-1β and IL-18, and recruit immune cells to the site of exposure [23, 24]. The adaptive immune system may also be activated, particularly if nanoparticles act as haptens by binding to proteins and forming complexes that can trigger antibody production or T-cell activation. Such immune recognition can be advantageous—for example, in vaccine adjuvant design—or detrimental, leading to hypersensitivity or autoimmune reactions [25-27]. Therefore, regulating the immune-modulatory properties of nanoparticles is essential to ensuring their safe and effective use in biomedical and industrial applications.

Despite the promising potential of TiO_2 NPs and the protective properties of eugenol, comprehensive in vivo studies evaluating their combined effects on cytotoxicity and inflammation remain limited. The route of administration plays a critical role in shaping the biodistribution and toxicological profile of nanoparticles; however, many existing studies rely primarily on in vitro assays or assess only a single biological endpoint. Although various investigations have characterized phytochemical–nanoparticle conjugates or explored TiO_2-induced toxicity in vitro, relatively few have provided an integrated, in vivo, head-to-head comparison of a free phytochemical versus the same compound delivered through an inorganic nanocarrier. Additionally, much of the previous work has been restricted either to physicochemical characterization or to isolated biological assessments. In this study, we combine (i) a reproducible eugenol functionalization of TiO_2 supported by comprehensive physicochemical

characterization (TEM, XRD, FTIR, DLS/zeta potential), (ii) in vitro release profiling with kinetic analysis under physiologically relevant pH conditions, and (iii) a 14-day in vivo comparison of free eugenol and TiO_2-loaded eugenol in liver, kidney, and spleen using histopathology, systemic cytokine profiling, apoptosis assays, and gene expression analysis of the Nrf2/HO-1 antioxidant axis. By integrating physicochemical, pharmacological, and mechanistic endpoints, our work provides a more translationally relevant evaluation of the potential advantages and safety profile of eugenol delivery via TiO_2 nanoparticles. This research aims to investigate the comparative effects of free TiO_2 NPs and eugenol-loaded TiO_2 NPs on cytotoxicity and inflammatory responses following intraperitoneal administration in a murine model. By elucidating how eugenol modulates the biological behavior of TiO_2 NPs, this study contributes to the development of safer nanoparticle designs for biomedical and industrial applications. Furthermore, it adds to the growing body of evidence supporting the incorporation of plant-derived compounds in nanomedicine to balance therapeutic efficacy with improved biocompatibility.

MATERIALS AND METHODS

TiO_2 NPs synthesis and characterization

Titanium dioxide nanoparticles (TiO_2 NPs) were synthesized via a co-precipitation method using analytical-grade reagents without further purification. Titanium tetrachloride ($TiCl_4$) and sodium hydroxide (NaOH) were mixed at a 1:1 molar ratio under ambient conditions. The resulting white precipitate was collected by centrifugation, thoroughly washed with distilled water, and filtered through cellulose nitrate membranes. The purified product was then dried at room temperature for 24 hours and subsequently sintered at 100 °C for an additional 24 hours. Characterization of TiO_2 NPs was performed using Fourier-transform infrared spectroscopy (FTIR), X-ray diffraction (XRD), dynamic light scattering (DLS), zeta potential analysis, field-emission scanning electron microscopy (FE-SEM), and transmission electron microscopy (TEM).

Eugenol loading onto TiO_2 NPs

For drug loading, following the eugenol calibration assay, 100 mg of synthesized TiO_2 NPs was incubated with 50 mg of eugenol under continuous magnetic stirring at ambient temperature in the dark for 24 hours. After centrifugation (10,000 rpm for 10 min), the supernatant was collected to determine the loading efficiency. The precipitate, which contained the eugenol-loaded TiO_2 NPs, was stored at −20 °C for subsequent analyses. The amount of free eugenol in the supernatant was quantified using UV–Vis spectrophotometry at 280 nm after appropriate dilution. A standard calibration curve was constructed, and the drug-loading efficiency was calculated using the equation below and further confirmed by FTIR and zeta potential analysis.

$$\textbf{Efficacy of loaded drug\%} = \frac{\textbf{Initial drug Concentration} - \textbf{Concentration of unloaded drug}}{\textit{Initial drug concentration}} \times \mathbf{100}$$

Evaluation of drug release in vitro

The release of eugenol was evaluated in PBS solutions at pH 7.2 and pH 4 using the dialysis bag diffusion method. Eugenol-loaded TiO_2 NPs (40 mg) were suspended in 500 µL of PBS and sealed within dialysis membranes. Each dialysis bag was immersed in 20 mL of the corresponding PBS solution and shaken at 100 rpm. At predetermined time intervals (0.5, 1, 2, 4, 6, 8, 10, 12, 24, and 48 h), a 1-mL aliquot of the release medium was withdrawn and replaced with an equal volume of fresh PBS. The amount of eugenol released was quantified using UV–Vis spectroscopy at 280 nm, and the cumulative release (%) was calculated accordingly.

In vivo animal model

Thirty-six adult male BALB/cJ mice were selected for the study. All animals were similar in age (6–8 weeks) and body weight (18–20 g) to ensure consistency across experimental subjects. The mice were obtained from the Royan Institute for Biotechnology animal facility in Isfahan, Iran. They were provided with a standard rodent diet and had unrestricted access to water. To mimic natural conditions, the animals were housed at 25 ± 2 °C with a 12-hour light/dark cycle, and the relative humidity was maintained at 55 ± 5%. Before the experiment, the mice were allowed a one-week acclimatization period. All experimental procedures followed international guidelines for the care and use of laboratory animals and were approved by the Institutional Animal Ethics Committee of Shahrekord University (Code: IR.SKU.REC.1403.039). The mice were randomly assigned to six experimental groups (n = 6 per group) and received daily treatments at 9:00 a.m. for 14 consecutive days. The Control group consisted of healthy mice that received an intraperitoneal (i.p.) injection of 100 µL deionized distilled water, which served as the vehicle for both TiO_2 NPs and Eugenol-loaded TiO_2 NPs (TiO_2@Eugenol). The Eugenol group received an i.p.

injection of eugenol at 20 mg/kg body weight, dissolved in 1 mL of deionized distilled water; this dosage was selected based on previous studies in mice [28-31]. The Low-dose TiO_2 NPs group received 50 mg/kg body weight of TiO_2 NPs administered i.p. in 1 mL deionized distilled water, while the High-dose TiO_2 NPs group received 200 mg/kg body weight of TiO_2 NPs prepared in the same vehicle. The Low-dose TiO_2@Eugenol group received 50 mg/kg body weight of eugenol-loaded TiO_2 NPs, and the High-dose TiO_2@Eugenol group was administered 200 mg/kg body weight of the same formulation.

Tissue and serum collection

After the 14-day treatment period, all animals were fasted overnight. The following morning, they were necropsied under mild anesthesia to minimize pain and stress. Blood samples were collected via cardiac puncture and immediately processed by centrifugation. The samples were centrifuged at 1500 g for 10 minutes at 4 °C to obtain serum, which was then promptly stored at −80 °C for subsequent immunological analyses. The liver, kidney, and spleen were carefully excised from each animal. Tissue samples were collected for detailed microscopic evaluation and cytotoxicity assessments. The liver and spleen were mechanically homogenized with a tissue homogenizer, and the homogenates were centrifuged to separate cellular components by density. The resulting supernatants were stored at −80 °C, a temperature appropriate for maintaining biomolecular integrity for future analyses.

ELISA analyze

The enzyme-linked immunosorbent assay (ELISA) was performed to determine serum levels of the inflammatory cytokines IL-6, IL-1β, and TNF-α. Undiluted serum samples and standard solutions were added to the microplate wells and incubated with gentle shaking for two hours at room temperature. After incubation, the wells were washed five times with the washing buffer. A conjugated detection antibody was then added, followed by a one-hour incubation, and the wells were rewashed. Subsequently, the HRP–avidin reagent was added and incubated for 30 minutes. After a final wash, the substrate solution was added, and the reaction was allowed to proceed for 10 minutes before the stop solution was applied. Absorbance was measured at 450 nm using a microplate reader, and cytokine concentrations were quantified using a calibration curve generated from standard solutions.

Assessment of Caspase-3/7 activity

A colorimetric Caspase-3/7 Assay Kit based on the hydrolysis of the Ac-DEVD-pNA substrate—which releases p-nitroaniline (pNA) detectable at 405 nm—was used to measure caspase-3 and caspase-7 activities. Briefly, approximately 40 mg of tissue was lysed in Caspase Lysis Buffer using sonication or homogenization, and the lysates were centrifuged at 12,000 rpm for 15 minutes at 4 °C. The resulting supernatants were immediately stored at −80 °C until further analysis. A calibration curve was generated using a series of pNA standards (0–50 µM). For the assay, 50 µL of each sample, standard, or positive control was added in duplicate to a 96-well microplate. A working solution containing Caspase Buffer, DTT, and the DEVD-pNA substrate (55.5 µL per well) was then added, and the plate was incubated at 37 °C for 1.5–2 hours. Absorbance was measured at 405 nm using a microplate reader. Caspase activity was calculated based on the standard curve and expressed as nmol/min/mL (mU/mL).

qRT-PCR analysis

Total RNA was extracted from liver tissue using TRIzol reagent, and cDNA was synthesized using an M-MLV Reverse Transcription Kit with random hexamers and oligo(dT) primers. The resulting cDNA was stored at −20 °C until further analysis. For quantitative real-time PCR (qPCR), gene-specific primers were designed for the housekeeping gene and for oxidative stress–related genes (SOD3, GPx, and GR). Primer sequences are presented in Table 1. Each 10 µL qPCR reaction consisted of 5 µL Takara SYBR Green Master Mix, 0.6 µL of 10 µM forward and reverse primers, 1.2 µL cDNA, and 3 µL RNase-free water. The thermal cycling protocol included an initial denaturation at 95 °C for 5 minutes, followed by 40 cycles of denaturation at 95 °C for 10 seconds, annealing at 58 °C for 15 seconds, and extension at 72 °C for 10 seconds. A melt-curve analysis was performed from 64 °C to 95 °C to verify amplicon specificity. Relative gene expression levels were calculated using the ΔΔCt method, with ACTB serving as the internal reference gene.

Table1. Mouse qPCR forward and reverse primer sequences

Gene name	Sequence	Product size
F-mACTB	5′- GGACTCCTATGTGGGTGACG-3′	119 bp
R-mACTB	5′- AGGTGTGGTGCCAGATCTTC-3′	
F-mGpx	5′-AATACCTTGAACTGAATGCAC-3′	111 bp
R-mGpx	5′-GAGTTCTCGCCTGGCTCCTG-3′	
F-mSOD3	5′- TTGACCCGGTTGAGAAGATAG-3′	121 bp
R-mSOD3	5′- ATCTCGGCAGCATCCACCTC-3′	
F-mGR	5′- GGCAGCTCCATCTCAGTCCG -3-	126 bp
R-mGR	5′- CTTTCAGGGCACTTGGTACTC-3′	

Statistical analysis

All experiments were performed in triplicate. Statistical analyses were conducted using Student's t-test and one-way ANOVA, followed by appropriate post hoc tests. Differences were considered statistically significant at $p < 0.05$.

RESULTS

Description of TiO_2 NPs

The synthesis of titanium dioxide (TiO_2) nanoparticles was performed using a precipitation method. The FTIR spectrum (Figure 1A) showed a broad absorption band between 450 and 800 cm^{-1}, corresponding to the stretching vibrations of Ti–O and Ti–O–Ti bonds. A peak at 1120 cm^{-1} was attributed to the stretching modes of C–O, C–N, and CH_3 groups, while the peak at 1380 cm^{-1} was explicitly associated with CH_3 stretching. The band observed at 1628 cm^{-1} indicated the presence of hydroxyl groups on the nanoparticle surface. XRD analysis (Figure 1B) confirmed the crystalline nature and polymorphism of the TiO_2 NPs. The diffraction pattern displayed characteristic reflections corresponding to the (101), (004), (200), (211), (204), (220), (215), and (312) planes, consistent with the presence of anatase and rutile phases, both commonly observed in TiO_2 nanoparticle structures. DLS measurements revealed an average hydrodynamic diameter of 73.8 nm with a polydispersity index (PDI) of 0.38 (Figure 1C), indicating a relatively narrow size distribution suitable for predictable biological and physicochemical behavior. The zeta potential of −44 mV (Figure 1D) demonstrated strong colloidal stability and uniform dispersion in aqueous media. FE-SEM imaging (Figure 1E) showed that the TiO_2 NPs were predominantly spherical, with uniform morphology and distribution at a magnification scale of 500 nm. TEM analysis (Figure 1F) further confirmed the spherical architecture of the nanoparticles, revealing a slightly roughened surface at the 100 nm scale.

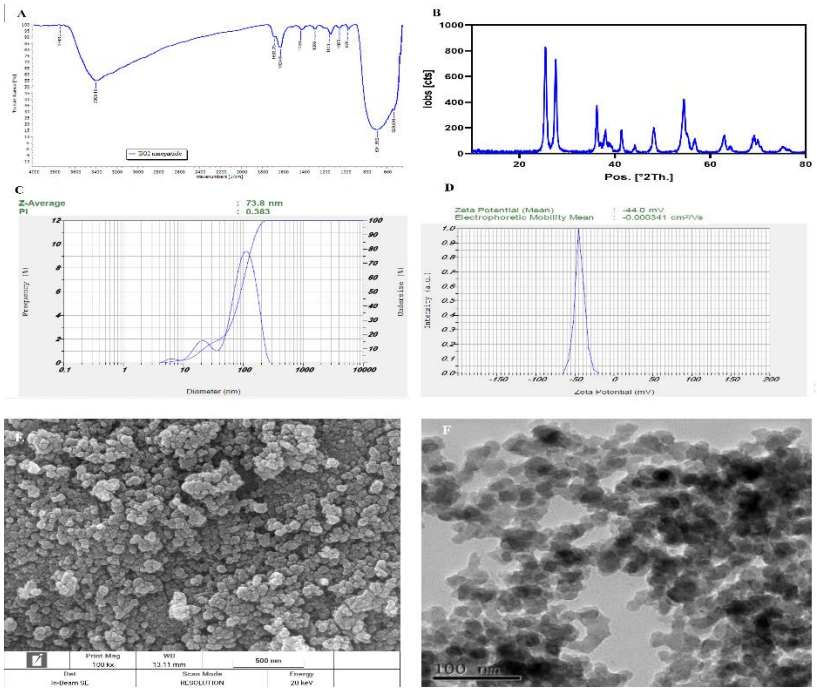

Fig. 1. TiO_2 NPs characterization. A) FTIR spectra of TiO_2 NPs, B) XRD pattern of TiO_2 NPs, C) Size and PDI of TiO_2 NPs determined to be 73.8 nm and 0.383, respectively, through DLS, D) Zeta potential of TiO_2 NPs obtained using the Zetasizer and found to be -44 mV. E) FE-SEM images of TiO_2 NPs to identify the surface morphology. The scale bars used here is 500 nm. F) TEM image of TiO_2 NPs. The scale bar used here is 100 nm.

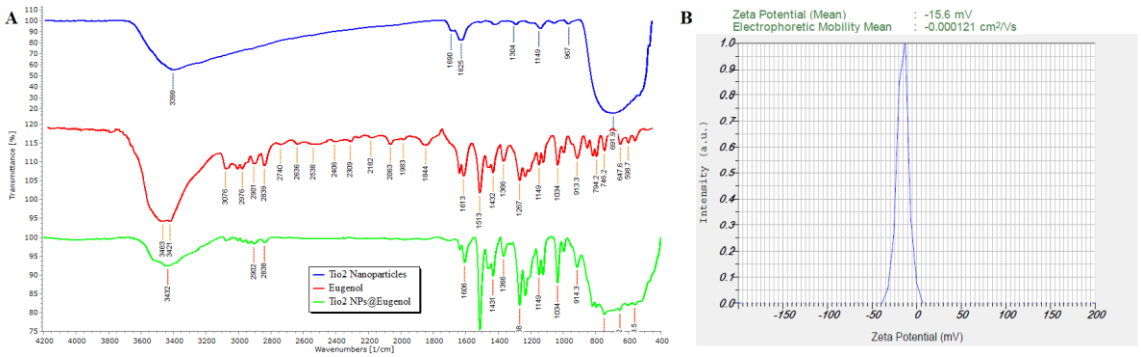

Fig. 2. TiO_2@Eugenol characterization indicating the successful loading of eugenol into TiO_2 NPs. A) FTIR spectra of TiO_2 NPs, eugenol, and TiO_2@Eugenol B) Zeta potential of TiO_2@Eugenol obtained using the Zeta sizer and found to be -15.6 mV.

Loading efficiency of eugenol

The eugenol loading efficiency was 99.4%. To verify the successful loading of eugenol onto the nanoparticles, FTIR and zeta potential analyses were conducted. The results of these assessments are shown in Figures 2A and 2B, respectively. Zeta potential measurements revealed a marked reduction in the negative surface charge of the nanoparticles—from −44 mV to −15 mV—confirming the presence of eugenol on the nanoparticle surface. Consistently, the FTIR spectrum of the loaded nanoparticles displayed overlapping characteristic peaks of both pure TiO_2 NPs and pure eugenol, indicating effective incorporation of eugenol. The absence of additional peaks suggests that no new chemical bonds or compounds were formed during loading.

Eugenol release results

As shown in Figure 3, a clear difference was observed between the release profiles of eugenol at pH 5.5 and pH 7.4 (the latter mimicking physiological conditions). In both media, the cumulative release increased over time, indicating sustained release over the 48 hours. The release rate was consistently higher under neutral conditions compared to acidic conditions, confirming the pH-responsive behavior of the TiO_2 nanoparticles. After approximately 8 hours, the release rate increased in both environments, with a more pronounced difference emerging between neutral and acidic media. At pH 7.4, eugenol release continued to rise gradually, reaching approximately 68% at 24 hours, followed by a plateau phase. In contrast, at pH 5.5, release occurred more slowly, reaching about 52% at 24 hours before stabilizing. Kinetic modeling of the release data indicated that the Higuchi model provided the best fit (R^2 = 0.97), suggesting a diffusion-controlled release mechanism.

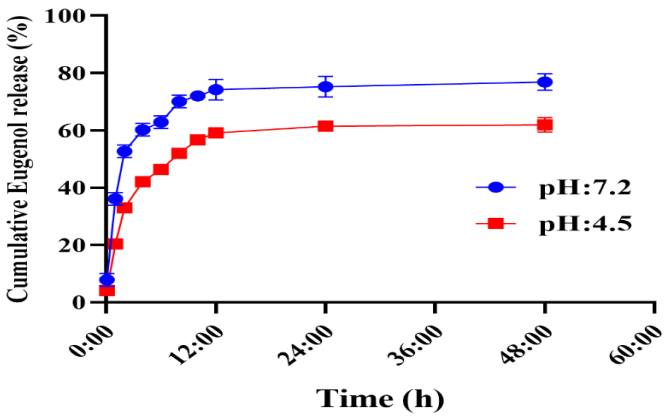

Fig. 3. Eugenol release profile over 48 hours at pH 4.5 (red curve) and pH 7.2 (blue curve).

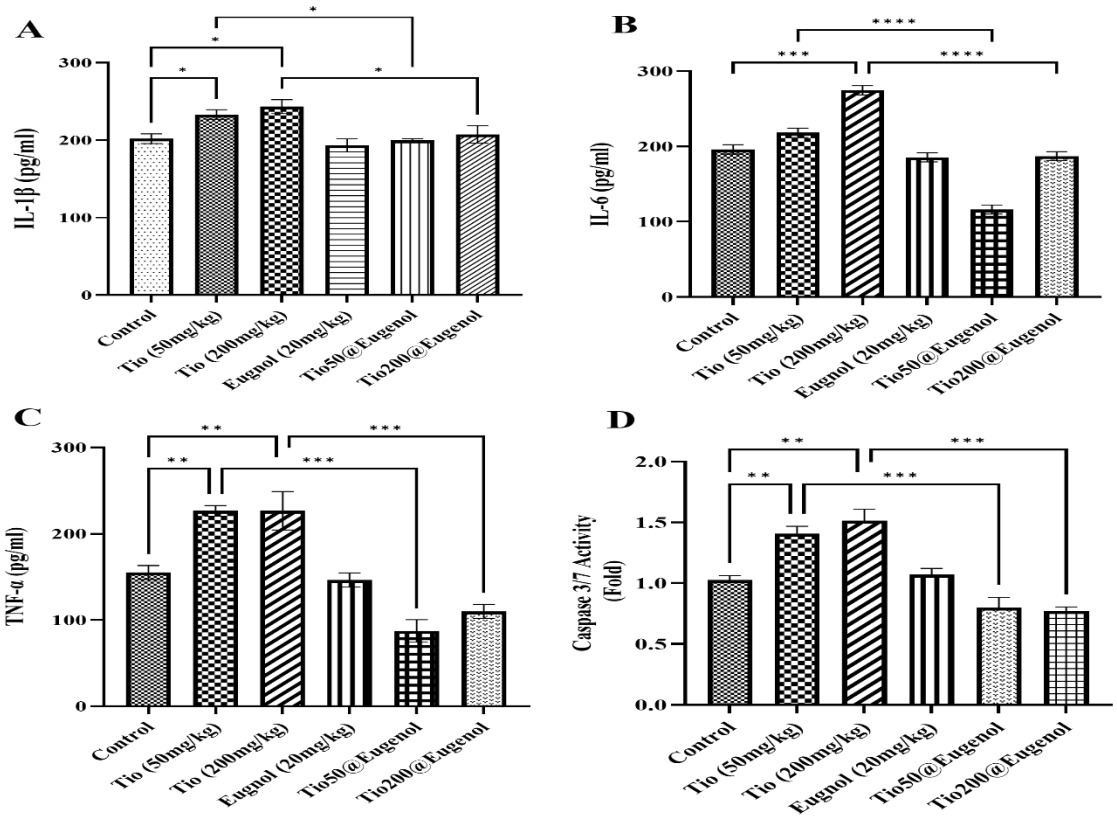

Fig. 4. ELISA assay results. Levels of (A) IL-1β, (B) IL-6, and (C) TNF-α D) Caspase 3/7 assay results, under individual and co-treatment with TiO2 NP, Eugenol and TiO2@Eugenol. *P < 0.05, ** P < 0.01, and *** P < 0.001, and **** indicate P < 0.0001

Assessment of inflammatory factors in serum

To quantify the inflammatory interleukins TNF-α, IL-1β, and IL-6 in serum samples from treated mice, an ELISA assay was performed (Figure 4). Analysis of IL-1β levels showed a significant dose-dependent increase in mice treated with TiO_2 NPs. In contrast, mice receiving eugenol-loaded NPs exhibited a marked reduction in IL-1β levels. This decrease was comparable between the two eugenol-loaded NP treatment groups (50 and 200 mg/kg).

Another inflammatory interleukin assessed in this study was IL-6. In mice treated with a high dose of TiO_2 NPs (200 mg/kg), IL-6 levels increased markedly, approximately 1.2-fold ($P < 0.001$). In contrast, treatment with TiO_2@eugenol reduced IL-6 levels, with the 50 mg/kg dose producing a greater decrease than the 200 mg/kg dose. Mice receiving eugenol alone also exhibited lower IL-6 levels, further supporting its anti-inflammatory effect.

In addition to assessing inflammatory interleukins, TNF-α levels were also evaluated. The analysis revealed a significant elevation in serum TNF-α in mice treated with both the low and high doses of TiO_2 NPs ($P < 0.001$). In contrast, mice receiving TiO_2@eugenol showed a marked reduction in TNF-α levels at both concentrations. Notably, compared with the nanoparticle-treated groups, the TiO_2@eugenol-treated mice exhibited nearly a twofold decrease in TNF-α levels. A similar reduction was also observed in mice treated with eugenol alone, further confirming its anti-inflammatory activity.

Evaluation of Caspase-3/7 activity

Another parameter evaluated in this study was caspase activity in liver extract samples from mice treated with either TiO_2 NPs alone or eugenol-loaded NPs. The results showed that caspase-3/7 activity increased by approximately 1.5-fold and 1.8-fold in mice treated with 50 and 200 mg/kg of TiO_2 NPs, respectively. In contrast, treatment with TiO_2@eugenol at 50 mg/kg resulted in a substantial reduction in caspase activity compared with TiO_2 NPs alone ($P < 0.0001$). A decrease in caspase activity was also observed in mice treated with TiO_2@eugenol at 200 mg/kg, although this reduction did not reach statistical significance. Overall, eugenol-loaded NPs demonstrated a pronounced inhibitory effect on caspase-3/7 activity.

Histological analysis of liver, kidney, and spleen

To evaluate the effects of the nanoparticles on inflammation and tissue damage, liver, spleen, and

kidney specimens were collected from treated mice. The samples were stained with hematoxylin and eosin (Figures 5, 6, and 7), and the extent of tissue alterations was examined. Histopathological analysis revealed that treatment with TiO_2 NPs at doses of 50 and 200 mg/kg led to a marked increase in necrosis and inflammation in hepatic tissue, the red and white pulp regions of the spleen, and renal tissue. In contrast, mice treated with eugenol-loaded NPs exhibited considerably reduced inflammation and necrosis. Liver sections from these groups displayed tissue morphology comparable to that of normal controls, and spleen samples also demonstrated significantly lower levels of structural damage and inflammatory infiltration.

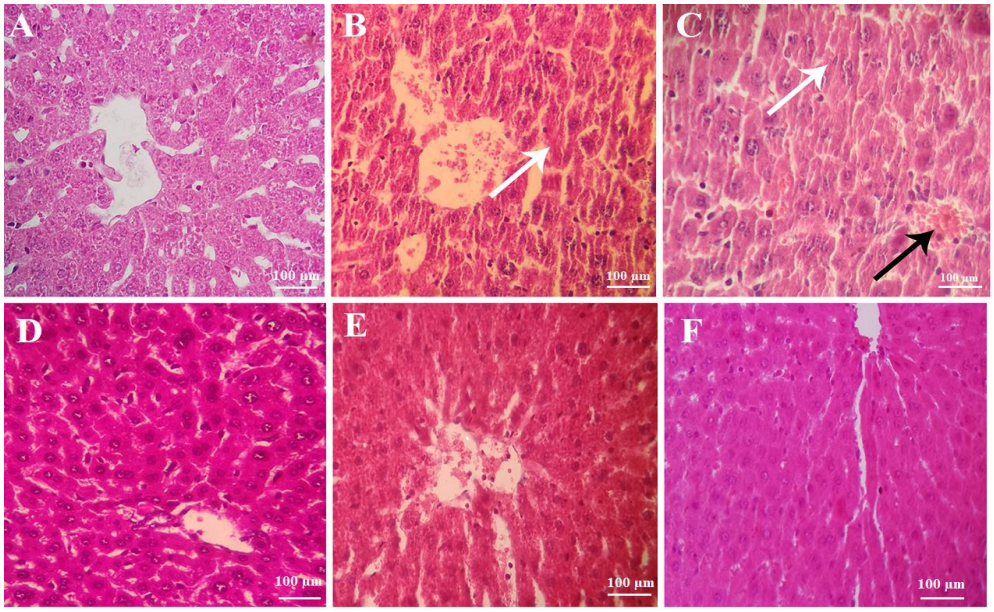

Fig. 5. Pathological Analysis of Liver Tissue: (A) Liver sample from the control group. (B) Liver sample from the group treated with 50 mg/kg of NPs, showing hepatocyte necrosis (indicated by the white arrow). (C) Liver sample treated with 200 mg/kg of NPs, displaying hepatocyte necrosis (white arrow) and central vein congestion (black arrow). (D) Liver sample from the eugenol treated group, where cells appear in normal condition. (E) Liver sample treated with eugenol-loaded NPs at 50 µg, with cells in a normal state. (F) Liver sample treated with eugenol-loaded NPs at 200 mg/kg, showing no hemorrhage or necrosis in the liver tissue.

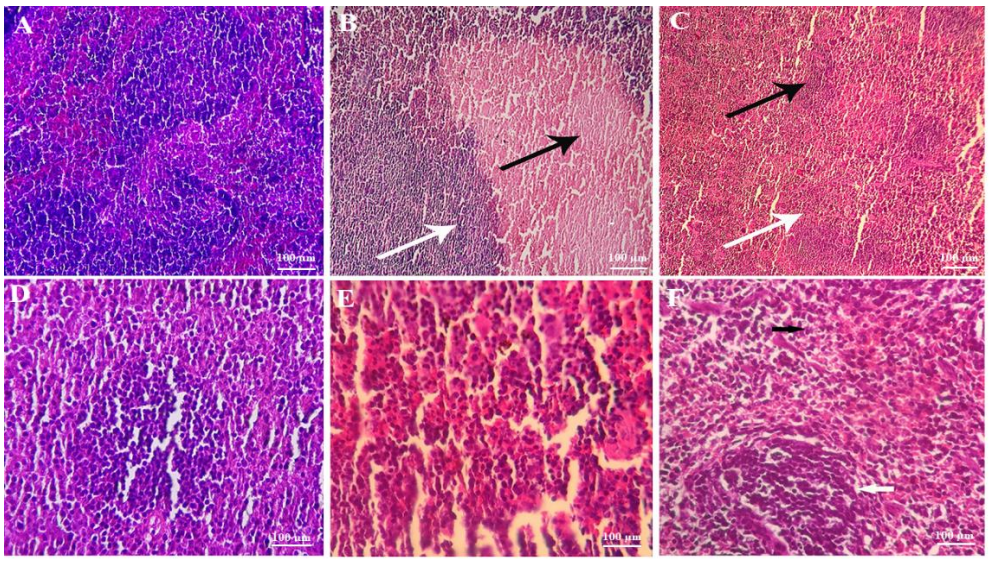

Fig. 6. Pathological Analysis of Spleen Tissue: (A) Spleen sample from the control group. (B) Spleen sample from the group treated with 50 µg of NPs, showing pulp necrosis (black arrow) and inflammation (white arrow). (C) Spleen sample treated with 200 µg of NPs, displaying necrosis in both red and white pulp (black and white arrows). (D) Spleen sample from the eugenol-treated group, where cells appear in normal condition. (E) Spleen sample treated with eugenol-loaded NPs at 50 µg, showing reduced necrosis compared to NPs alone. (F) Spleen sample treated with eugenol-loaded NPs at 200 µg, with decreased necrosis and clearly distinguishable red and white pulp.

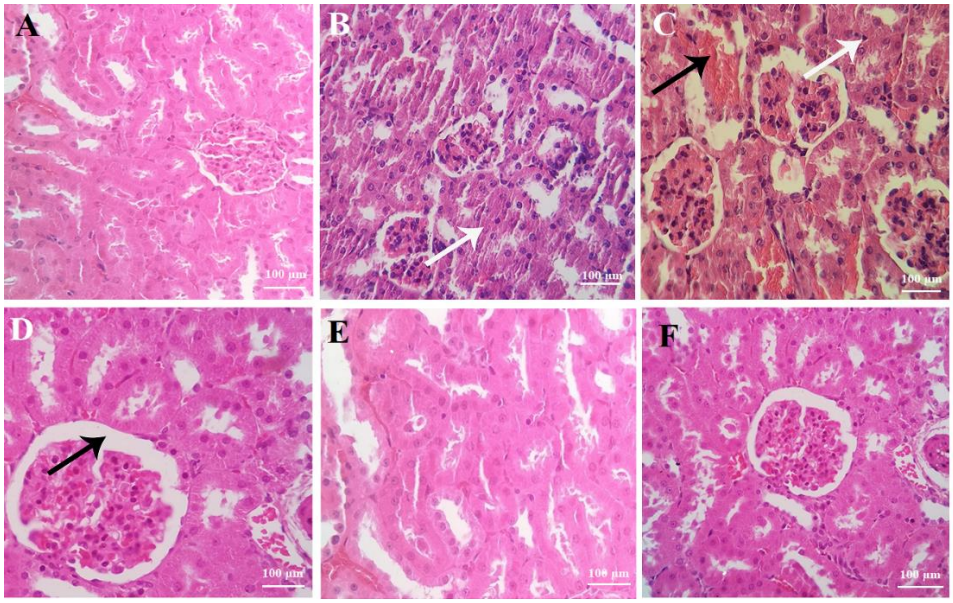

Fig. 7. Pathological Analysis of Kidney Tissue: (A) Kidney sample from the control group. (B) Kidney sample from the group treated with 50 µg of NPs, showing degeneration of renal tubular cells (white arrow). (C) Kidney sample treated with 200 µg of NPs, displaying degeneration of kidney cells (white arrow) and hemorrhage (black arrow). (D) Kidney sample from the eugenol treated group, where cells appear in normal condition, with an enlargement of Bowman's space. (E) Kidney sample treated with eugenol-loaded NPs at 50 µg, where cells are in a normal state. (F) Kidney sample treated with eugenol loaded NPs at 200 µg, showing normal kidney tissue, renal tubules, and glomeruli.

Real-time quantitative data analysis

As illustrated in Figure 8, treatment with bare TiO_2 NPs at concentrations of 50 µg and 200 µg induced an apparent reduction in the expression of transcripts encoding antioxidant enzymes, including SOD3, GR, and GPx. The extent of gene suppression was dose-dependent, with significantly greater inhibition observed at the higher concentration ($P < 0.01$), indicating potential pro-oxidant effects of bare NPs at elevated doses. In contrast, administration of eugenol alone or eugenol-loaded NPs resulted in a pronounced upregulation of these antioxidant-related genes. Specifically, liver tissues exposed to eugenol-loaded NPs exhibited a 1.7-fold increase in SOD3 expression, along with 1.5-fold and 1.2-fold increases in GR and GPx, respectively, compared with untreated controls and bare NP-treated groups. Notably, no statistically significant differences were observed between the 50 µg and 200 µg doses of eugenol-loaded NPs, suggesting a saturation effect or a potential upper limit in transcriptional activation within this dosage range. Collectively, these findings highlight eugenol's protective role against NP-induced oxidative stress and underscore its potential to modulate redox homeostasis at the molecular level through eugenol-functionalized nanocarriers.

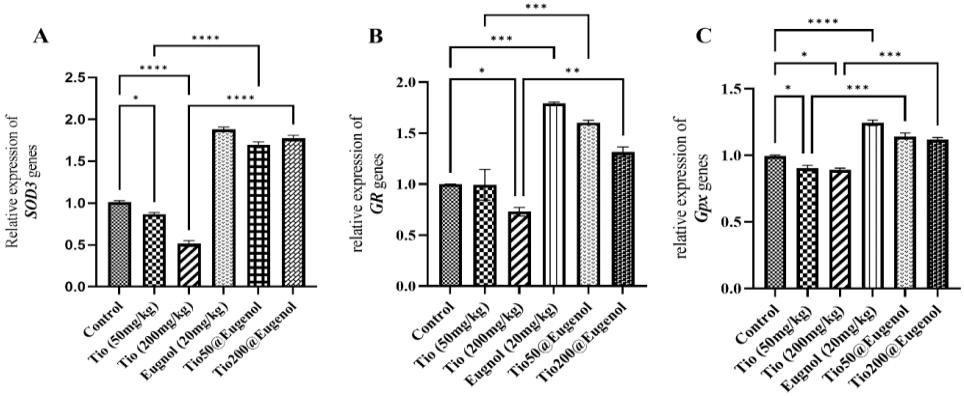

Fig. 8. Gene expression changes of SOD3, GR, and GPx under treatments with titanium dioxide NPs alone, eugenol alone, and eugenol-loaded NPs. Statistical significance of expression differences is shown in comparison to the control group and between loaded and single treatments: *p<0.01, **: p<0.001, ***: p<0.0001, ****: P<0.00001.

DISCUSSION

With the expanding use of TiO_2 nanoparticles (TiO_2 NPs) in industrial and consumer products, human exposure has become increasingly unavoidable, leading to their accumulation in various organs. Such accumulation has been linked to oxidative damage, apoptosis, genotoxicity, and chromosomal instability [32, 33]. In the present study, we investigated the inflammatory, oxidative, and histopathological effects of TiO_2 NPs in their bare form and when functionalized with eugenol.

TiO_2 NP exposure is well documented to induce the production of inflammatory cytokines, primarily by activating immune cell responses and key inflammatory signaling pathways. TiO_2 NPs disrupt the inhibitory function of IκB, thereby facilitating NF-κB translocation into the nucleus and promoting the transcriptional upregulation of major inflammatory cytokines. This mechanism has been reported across multiple organs, including the lungs and brain, underscoring the systemic nature of TiO_2 NP–induced inflammation [34, 35]. In addition to NF-κB activation, TiO_2 NPs enhance the expression of Toll-like receptors (TLRs), particularly TLR2 and TLR4, on the surface of immune cells. These receptors are critical components of the innate immune system, recognizing pathogen-associated molecular patterns and amplifying downstream inflammatory signaling. Their upregulation further intensifies NF-κB activation, thereby contributing to the increased cytokine production observed following nanoparticle exposure [36].

The immune response to TiO_2 NPs also triggers the recruitment of inflammatory cells, primarily neutrophils and macrophages. These cells infiltrate affected tissues and secrete additional cytokines, creating a self-sustaining inflammatory loop that intensifies tissue damage [37]. Histopathological evaluations in multiple studies have confirmed such immune cell infiltration in organs exposed to TiO_2 NPs. Furthermore, TiO_2 NPs induce tissue-specific inflammation in organs such as the lungs, heart, and brain, resulting in observable structural damage. The extent and pattern of inflammation vary across organs, suggesting differential susceptibility and distinct response mechanisms [37-40]. Another essential aspect of TiO_2 NP-induced immunotoxicity is the disruption of the Th1/Th2 cytokine balance. Exposure to these nanoparticles tends to shift the immune response toward a Th1-dominant profile, accompanied by elevated transcriptional activation of inflammatory cytokines such as IL-1β and TNF-α. This imbalance may further potentiate chronic inflammation and contribute to long-term immune dysregulation [37].

In contrast, eugenol-loaded NPs significantly attenuated this inflammatory response, even at higher concentrations. The anti-inflammatory effects of eugenol, particularly when delivered via nanoparticles, arise from a combination of molecular and cellular mechanisms that synergistically modulate inflammatory signaling. A central aspect of eugenol's activity is the downregulation of key pro-inflammatory mediators. It markedly suppresses cytokine production and, subsequently, reduces the synthesis of critical inflammatory factors, such as nitric oxide (NO) and prostaglandins, thereby dampening the inflammatory cascade [41-43]. In addition to its immunomodulatory properties, eugenol possesses potent antioxidant activity. By effectively neutralizing reactive oxygen species (ROS), including superoxide and hydroxyl radicals, it mitigates oxidative stress—a well-established trigger of inflammatory signaling pathways. This reduction in ROS levels stabilizes cellular redox balance, thereby limiting ROS-mediated injury and inflammation [44]. At the intracellular level, eugenol interferes with major inflammatory signaling pathways, most notably the NF-κB and MAPK cascades, including ERK1/2 and p38. Inhibition of these pathways results in decreased expression of inflammation-related genes and reduced recruitment of immune cells to sites of tissue injury [45]. Furthermore, eugenol modulates immune cell behavior by reducing leukocyte adhesion and migration into inflamed tissues. It also suppresses macrophage activation and the subsequent release of inflammatory mediators, all without exerting cytotoxic effects on immune cells. This targeted immunoregulation helps limit tissue damage while preserving normal immune function [44].

Another noteworthy finding was that low-dose eugenol exerted a stronger inhibitory effect on IL-6 levels and caspase-3/7 activity than the higher dose. This outcome may reflect a hormetic response, wherein low concentrations of phenolic compounds activate protective antioxidant and anti-inflammatory pathways. In contrast, higher concentrations may paradoxically induce mild oxidative stress and diminish overall efficacy. Similar biphasic dose-dependent effects of eugenol have been reported in previous studies [46, 47].

Apoptosis analysis by caspase-3/7 activity revealed a notable increase in hepatic caspase activation following TiO_2 exposure, reaching up to 1.8-fold at 200 mg/kg, consistent with the observed cytotoxic and inflammatory responses. In contrast,

caspase activity was significantly reduced in mice treated with eugenol-loaded NPs, particularly at the 50 mg/kg dose, supporting eugenol's protective role. Previous studies have demonstrated the accumulation of TiO_2 NPs in rat tissues following intraperitoneal administration, with toxicity mediated mainly by reactive oxygen species (ROS) [48, 49]. Treatment with eugenol-loaded NPs has been shown to substantially reduce caspase activation in hepatic cells by mitigating oxidative stress, suppressing inflammatory signaling, and preserving cellular membrane integrity. These interconnected mechanisms collectively protect hepatocytes against apoptosis during liver injury. A central protective mechanism is eugenol's antioxidant activity, which efficiently scavenges free radicals and reduces lipid peroxidation (LPO) in hepatic tissue. By reducing oxidative stress, eugenol helps prevent mitochondrial dysfunction—a key trigger of the intrinsic apoptotic pathway that leads to caspase activation, particularly caspase-3 [50]. In this study, free eugenol provided only modest protection against TiO_2-induced oxidative stress and inflammation. This limited therapeutic effect aligns with the known pharmacokinetic limitations of eugenol, including its low solubility, chemical instability, and rapid systemic clearance [51]. In contrast, TiO_2@eugenol NPs exhibited markedly stronger protective effects, evidenced by reduced levels of TNF-α, IL-1β, and IL-6; decreased caspase-3 and caspase-7 activity; and restored expression of antioxidant genes. These enhanced outcomes can be attributed to the nanoparticle-based delivery system, which improves eugenol stability, prolongs its bioavailability, and enables controlled release at the target site [52, 53]. Collectively, these findings underscore the therapeutic advantage of nanoparticle functionalization in maximizing the protective potential of phytochemicals such as eugenol.

A limitation of this study is the absence of biodistribution analysis, which prevents confirmation of the precise organ-specific accumulation of TiO_2 and TiO_2@eugenol nanoparticles. Such investigations are essential for more accurately correlating histological and molecular alterations with actual tissue exposure. Another limitation is the potential toxicity associated with high-dose eugenol. Although eugenol has demonstrated potent antioxidant and anti-inflammatory activities, several studies have reported that, at elevated doses, it may exert hepatotoxic and pro-oxidant effects [54, 55]. Therefore, caution is warranted when extrapolating the protective effects observed here to higher or chronic dosing regimens. Future work should include biodistribution studies, pharmacokinetic profiling, and long-term toxicity evaluations to more comprehensively assess safety. Another limitation is that caspase-3/7 activity was evaluated only in liver tissue. This decision was based on the well-established tendency of TiO_2 nanoparticles to preferentially accumulate in the liver following systemic exposure [56, 57], as well as the focus of our gene expression analysis on hepatic antioxidant pathways. However, apoptosis in other organs, such as the kidney and spleen, may also contribute to systemic toxicity. Future studies should therefore incorporate multi-organ apoptosis assessments to provide a more complete evaluation of both protective and adverse effects.

Moreover, eugenol treatment restores the activity of endogenous antioxidant defenses, including SOD and GPx, as well as reduced glutathione (GSH) levels. This restoration of redox balance contributes to cellular stability and inhibits oxidative signals that drive apoptotic cascades [58]. In addition to its antioxidant effects, eugenol exerts significant anti-inflammatory activity by suppressing the production of inflammatory mediators that are known to be elevated during hepatic inflammation and injury. Because these cytokines play a critical role in promoting apoptotic signaling—particularly through extrinsic pathways—their downregulation leads to reduced caspase activation and diminished hepatocyte death [59]. Eugenol also plays an essential role in membrane stabilization, preserving the structural integrity of hepatocyte membranes and limiting cellular leakage and damage. This membrane-protective action reduces stimuli that trigger apoptotic signaling and further contributes to hepatoprotection [60]. Notably, both in vitro and in vivo studies have demonstrated that eugenol directly modulates apoptotic pathways by reducing caspase-3 expression and activity, a key executioner enzyme in the apoptotic process. The use of nanoparticles as a delivery system enhances these protective effects by improving eugenol's bioavailability and cellular uptake, thereby amplifying its therapeutic potential [59, 61].

Histological examination of the liver, spleen, and kidney further confirmed the systemic toxicity of TiO_2 NPs. Pronounced necrosis, hemorrhage, and inflammatory cell infiltration were evident in all three organs. Consistent with these findings, Liu et al. (2009) also reported substantial TiO_2 NP accumulation in the liver of mice [62]. In contrast, mice treated with eugenol-functionalized NPs exhibited markedly attenuated pathological alterations. Hepatic architecture, renal tubular structures, and splenic tissue displayed near-normal

morphology, underscoring the enhanced biocompatibility and therapeutic potential of eugenol-loaded NPs. TiO_2 NPs induce toxicity primarily through oxidative stress, generating ROS that drive lipid peroxidation, glutathione depletion, reduced antioxidant enzyme activity, DNA damage, and inflammation in vital organs such as the liver, kidney, and spleen. These molecular effects are accompanied by elevated biochemical markers (e.g., ALT, ALP) and histological indicators of tissue injury. Functionalization of TiO_2 NPs with eugenol substantially mitigated these toxic manifestations. Eugenol reduced lipid peroxidation, restored antioxidant defenses (e.g., GSH, SOD, GPx), decreased DNA damage, and normalized liver and kidney function markers. Furthermore, it improved mitochondrial integrity and reduced blood cell cytotoxicity [63]. At the molecular level, real-time PCR analysis revealed significant downregulation of key antioxidant genes (SOD3, GR, GPx) in animals treated with TiO_2 NPs, particularly at higher doses, supporting oxidative stress as a major mechanism of TiO_2-induced toxicity. In contrast, treatment with eugenol-loaded NPs resulted in robust upregulation of these antioxidant markers, with SOD3 expression increasing by 1.7-fold, GR by 1.5-fold, and GPx by 1.2-fold. One of the principal molecular mechanisms underlying eugenol's antioxidant and cytoprotective effects is its activation of the Nrf2/HO-1 antioxidant pathway [51]. This pathway plays a pivotal role in maintaining redox homeostasis by enhancing the expression of endogenous antioxidant enzymes and suppressing oxidative injury [64]. Under physiological conditions, nuclear factor erythroid 2 2-related factor 2 (Nrf2) is sequestered in the cytoplasm by its repressor, Kelch-like ECH-associated protein 1 (KEAP1), which targets it for ubiquitination and proteasomal degradation. Upon oxidative stress or eugenol exposure, structural modifications in KEAP1 prevent Nrf2 degradation, thereby stabilizing Nrf2 and promoting its nuclear translocation [64-66]. Among the downstream targets of Nrf2, heme oxygenase-1 (HO-1) serves as a critical effector. Activation of the Nrf2/HO-1 axis by eugenol reduces intracellular ROS levels, enhances antioxidant enzyme activity, and provides substantial protection against oxidative stress-induced apoptosis. These protective effects have been documented across various cell types, including pancreatic β-cells, hepatocytes, and immune cells, in which eugenol-mediated Nrf2 activation mitigates oxidative injury and promotes cell survival [66, 67]. Notably, experimental inhibition of Nrf2 abolishes eugenol's protective actions, further emphasizing the centrality of this pathway in mediating its antioxidant and cytoprotective effects [68].

CONCLUSION

Overall, this study's findings demonstrate that bare TiO_2 NPs induce pronounced inflammatory and oxidative effects, particularly at higher concentrations. However, incorporation of eugenol into these nanoparticles not only mitigates these adverse outcomes but also enhances their therapeutic profile by reducing inflammation, apoptosis, and oxidative stress. Additionally, nanoparticle-based delivery markedly improves the pharmacokinetic properties of eugenol, including its solubility, stability, and cellular uptake. This enhanced delivery facilitates greater tissue penetration and increases local eugenol concentrations, thereby augmenting its anti-inflammatory and antioxidant efficacy, as reported in various experimental models. These results highlight the value of functionalizing nanoparticles with bioactive compounds, such as eugenol, to enhance biocompatibility and therapeutic efficacy. Further investigations—particularly those employing chronic exposure models and translational or clinical settings—are warranted to validate these findings and refine dosing strategies for future biomedical applications.

Future studies should extend these findings beyond short-term exposure by incorporating chronic or repeated-dose models to better characterize the long-term safety and efficacy of TiO_2@eugenol NPs. Comprehensive pharmacokinetic and biodistribution analyses will also be essential for determining systemic availability, organ-specific accumulation, and clearance mechanisms. Additionally, evaluating these nanoparticles in disease-specific contexts—such as metabolic liver disease, fibrosis, or cancer—where oxidative stress and inflammation play central pathological roles may further clarify their therapeutic potential and translational relevance.

AUTHOR CONTRIBUTIONS

F. Al-Naffakh performed most of the experiments as part of his master's degree in Cellular and Molecular Biology. S. Reiisi coordinated the study, designed the experiments, performed data analysis, and revised the manuscript. N. Khalighi performed the NPs study and participated in intellectual discussions of the data. E. Moghtadaei Khorasgani performed pathological analysis.

AVAILABILITY OF DATA AND MATERIALS

The authors declare that all generated and analyzed data are included in the manuscript.

CONFLICT OF INTEREST

We certify that there is no conflict of interest with any financial organization.

ETHICS APPROVAL

This study is approved in accordance with international guidelines and ethical research principles (code: IR.SKU.REC.1403.039).

CONSENT FOR PUBLICATION

This article does not contain any person's data in any form.

FUNDING

No funding

ACKNOWLEDGMENTS

Grammarly and ChatGPT were used to improve the spelling, grammar, and overall English of the manuscript. These tools were not employed in the research design, data analysis, or the formulation of conclusions, or in any parts generally considered core requirements for authorship.

REFERENCES

1. McNeil SE. Nanotechnology for the biologist. J Leukoc Biol. 2005;78(3):585-594.
2. Nath D, Banerjee P. Green nanotechnology–a new hope for medical biology. Environ Toxicol Pharmacol. 2013;36(3):997-1014.
3. Chandoliya R, Sharma S, Sharma V, Joshi R, Sivanesan I. Titanium Dioxide Nanoparticle: A Comprehensive Review on Synthesis, Applications and Toxicity. Plants. 2024;13(21):2964.
4. Irshad MA, Nawaz R, Ur Rehman MZ, Adrees M, Rizwan M, Ali S, et al. Synthesis, characterization and advanced sustainable applications of titanium dioxide nanoparticles: A review. Ecotoxicol Environ Saf. 2021;212:111978.
5. Racovita AD. Titanium dioxide: structure, impact, and toxicity. Int J Environ Res Public Health. 2022;19(9):5681.
6. Kendall M, Holgate S. Health impact and toxicological effects of nanomaterials in the lung. Respirology. 2012;17(5):743-758.
7. Gao Y, Zhai H, She X, Si H. Quantitative structure-activity relationships; studying the toxicity of metal nanoparticles. Curr Top Med Chem. 2020;20(27):2506-2517.
8. del Pilar Chantada-Vázquez M, López AC, Bravo SB, Vázquez-Estévez S, Acea-Nebril B, Núñez C. Proteomic analysis of the bio-corona formed on the surface of (Au, Ag, Pt)-nanoparticles in human serum. Colloids Surf B Biointerfaces. 2019;177:141-148.
9. Lima T, Bernfur K, Vilanova M, Cedervall T. Understanding the lipid and protein corona formation on different sized polymeric nanoparticles. Sci Rep. 2020;10(1):1129.
10. Lee DS, Shin YK. Innate Immunity to Nanomaterials. Radionanomedicine. 2018:389-407.
11. Perciani CT, Liu LY, Wood L, MacParland SA. Enhancing immunity with nanomedicine: employing nanoparticles to harness the immune system. ACS Nano. 2020;15(1):7-20.
12. Tetley TD. Health effects of nanomaterials. Biochem Soc Trans. 2007;35(Pt 3):527-531.
13. Wu T, Tang M. Review of the effects of manufactured nanoparticles on mammalian target organs. J Appl Toxicol. 2018;38(1):25-40.
14. Park E-J, Park K. Oxidative stress and pro-inflammatory responses induced by silica nanoparticles in vivo and in vitro. Toxicol lett. 2009;184(1):18-25.
15. Tee JK, Ong CN, Bay BH, Ho HK, Leong DT. Oxidative stress by inorganic nanoparticles. Wiley Interdiscip Rev Nanomed Nanobiotechnol. 2016;8(3):414-438.
16. Domingues L, Carriello GM, Pegoraro GM, Mambrini GP. Synthesis of TiO2 nanoparticles by the solvothermal method and application in the catalysis of esterification reactions. An Acad Bras Cienc. 2024;96(suppl 3):e20240096.
17. Santos-Aguilar P, Bernal-Ramírez J, Vázquez-Garza E, Vélez-Escamilla LY, Lozano O, García-Rivas GJ, et al. Synthesis and Characterization of Rutile TiO(2) Nanoparticles for the Toxicological Effect on the H9c2 Cell Line from Rats. ACS Omega. 2023;8(21):19024-19036.
18. Barboza JN, da Silva Maia Bezerra Filho C, Silva RO, Medeiros JVR, de Sousa DP. An Overview on the Anti-inflammatory Potential and Antioxidant Profile of Eugenol. Oxid Med Cell Longev. 2018;2018:39-57.
19. Chaieb K, Hajlaoui H, Zmantar T, Kahla-Nakbi AB, Rouabhia M, Mahdouani K, et al. The chemical composition and biological activity of clove essential oil, Eugenia caryophyllata (Syzigium aromaticum L. Myrtaceae): a short review. Phytother Res. 2007;21(6):501-506.
20. Zari AT, Zari TA, Hakeem KR. Anticancer Properties of Eugenol: A Review. Molecules. 2021;26(23).
21. Nisar MF, Khadim M, Rafiq M, Chen J, Yang Y, Wan CC. Pharmacological Properties and Health Benefits of Eugenol: A Comprehensive Review. Oxid Med Cell Longev. 2021;2021:2497354.
22. Farrera C, Fadeel B. It takes two to tango: Understanding the interactions between engineered nanomaterials and the immune system. Eur J Pharm Biopharm. 2015;95(Pt A):3-12.
23. Boraschi D, Canesi L, Drobne D, Kemmerling B, Pinsino A, Prochazkova P. Interaction between nanomaterials and the innate immune system across evolution. Biol Rev. 2023;98(3):747-774.
24. Tsugita M, Morimoto N, Nakayama M. SiO 2 and TiO 2 nanoparticles synergistically trigger macrophage inflammatory responses. Part Fibre Toxicol. 2017;14:1-9.
25. Farrera C, Fadeel B. It takes two to tango: Understanding the interactions between engineered nanomaterials and the immune system. European Journal of Pharmaceutics and Biopharmaceutics. 2015;95:3-12.
26. Ghosh S, Bhattacherjee R, Banerjee D. Nanoparticles and adaptive immunity. Hum Immunol. 2022;25.
27. Ko C-N, Zang S, Zhou Y, Zhong Z, Yang C. Nanocarriers for effective delivery: Modulation of innate immunity for the management of infections and the associated complications. J Nanobiotechnology. 2022;20(1):380.

28. Basante-Romo M, Gutiérrez-M JO, Camargo-Amado R. Non-toxic doses of modified titanium dioxide nanoparticles (m-TiO2NPs) in albino CFW mice. Heliyon. 2021;7(3).
29. Kazimirova A, Baranokova M, Staruchova M, Drlickova M, Volkovova K, Dusinska M. Titanium dioxide nanoparticles tested for genotoxicity with the comet and micronucleus assays in vitro, ex vivo and in vivo. Mutat Res Genet Toxicol Environ Mutagen. 2019;843:57-65.
30. Alypoor S, Abdolmaleki A, Mamoudi F, Haghighat K, Soluki M. Evaluation of the Neuroprotective Effect of Eugenol on the Improvement of Sciatic Nerve Injury in Rats. Iran j toxicol. 2023;17(3):53-59.
31. Zhao Y-x, Wang D, Bais S, Wang H-x. Modulation of pro-inflammatory mediators by Eugenol in AlCl3 induced dementia in rats. 2019.
32. Baranowska-Wójcik E, Szwajgier D, Oleszczuk P, Winiarska-Mieczan A. Effects of titanium dioxide nanoparticles exposure on human health—a review. Biol Trace Elem Res. 2020;193(1):118-129.
33. Gilbert JD, Neubauer K, Byard RW. Macroscopic identification of visceral titanium pigment in an intravenous drug user. J Forensic Sci. 2021;66(5):2024-2028.
34. Ze Y, Sheng L, Zhao X, Hong J, Ze X, Yu X, et al. TiO2 nanoparticles induced hippocampal neuroinflammation in mice. PloS One. 2014;9(3):e92230.
35. Liu D, Zhou JL, Hong F, Zhang YQ. Lung inflammation caused by long-term exposure to titanium dioxide in mice involving in NF-κB signaling pathway. J Biomed Mater Res Part A. 2017;105(3):720-727.
36. Lehotska Mikusova M, Busova M, Tulinska J, Masanova V, Liskova A, Uhnakova I, et al. Titanium Dioxide Nanoparticles Modulate Systemic Immune Response and Increase Levels of Reduced Glutathione in Mice after Seven-Week Inhalation. Nanomaterials (Basel). 2023;13(4).
37. Hong F, Wang L, Yu X, Zhou Y, Hong J, Sheng L. Toxicological effect of TiO2 nanoparticle-induced myocarditis in mice. Nanoscale Res Lett. 2015;10(1):326.
38. Liu D, Zhou JL, Hong F, Zhang YQ. Lung inflammation caused by long-term exposure to titanium dioxide in mice involving in NF-κB signaling pathway. J Biomed Mater Res A. 2017;105(3):720-727.
39. Jeong J-S, Jegal H, Ko J-W, Kim J-W, Kim J-H, Chung E-H, et al. Titanium Dioxide Nanoparticle Exposure Provokes Greater Lung Inflammation in Females Than Males in the Context of Obesity. Int J Nanomed. 2025:5321-5336.
40. Lim J-O, Lee S-J, Kim W-I, Pak S-W, Moon C, Shin I-S, et al. Titanium dioxide nanoparticles exacerbate allergic airway inflammation via TXNIP upregulation in a mouse model of asthma. Int J Mol Sci. 2021;22(18):9924.
41. Barboza JN, da Silva Maia Bezerra Filho C, Silva RO, Medeiros JVR, de Sousa DP. An overview on the anti-inflammatory potential and antioxidant profile of eugenol. Oxid Med Cell Longev. 2018;2018(1):39-57.
42. Nisar M, Khadim M, Rafiq M, Chen J, Yang Y, Wan C. Pharmacological Properties and Health Benefits of Eugenol: A Comprehensive Review. Oxid Med Cell Longev. 2021: 2497354. 2021.
43. Kumar A, Siddiqi NJ, Alrashood ST, Khan HA, Dubey A, Sharma B. Protective effect of eugenol on hepatic inflammation and oxidative stress induced by cadmium in male rats. Biomed Pharm. 2021;139:111588.
44. Keshari R, Tharmatt A, Pillai MM, Chitkara D, Tayalia P, Banerjee R, et al. Eugenol-Loaded lipid Nanoparticles-Derived hydrogels ameliorate Psoriasis-like skin lesions by Lowering oxidative stress and modulating inflammation. ACS Pharmacol Transl Sci. 2024;7(11):3592-3606.
45. Leem H-H, Kim E-O, Seo M-J, Choi S-W. Antioxidant and anti-inflammatory activities of eugenol and its derivatives from clove (Eugenia caryophyllata Thunb.). J Korea Soc Food Sci Nutr. 2011;40(10):1361-1370.
46. Nagababu E, Rifkind JM, Boindala S, Nakka L. Assessment of antioxidant activity of eugenol in vitro and in vivo. Methods Mol Biol. 2010;610:165-180.
47. Pires Costa E, Maciel dos Santos M, de Paula RA, da Silva DA, Lopes RP, Teixeira RR, et al. Antioxidant and Anti-inflammatory Activity of Eugenol, Bis-eugenol, and Clove Essential Oil: An In Vitro Study. ACS omega. 2025;10(28):31033-31045.
48. Cui XueYan CX, Yin Jun YJ, Lin Ying LY, Li Na LN, Wang MeiZhen WM, Shen DongSheng SD. Towards a definition of harmless nanoparticles from an environmental and safety perspective. 2016.
49. Valentini X, Rugira P, Frau A, Tagliatti V, Conotte R, Laurent S, et al. Hepatic and renal toxicity induced by TiO2 nanoparticles in rats: a morphological and metabonomic study. J Toxicol. 2019;2019(1):5767012.
50. Zaky MY, Morsy HM, Abdel-Moneim A, Zoheir KM, Bragoli A, Abdel-Maksoud MA, et al. Anticancer potential of eugenol in hepatocellular carcinoma through modulation of oxidative stress, inflammation, apoptosis, and proliferation mechanisms. Discov Oncol. 2025;16(1):1080.
51. Ma L, Liu J, Lin Q, Gu Y, Yu W. Eugenol protects cells against oxidative stress via Nrf2. Exp Ther Med. 2021;21(2):107.
52. Pramod K, Ansari SH, Ali J. Eugenol: a natural compound with versatile pharmacological actions. Nat Prod Commun. 2010;5(12):1934578X1000501236.
53. Chowdhury S, Nath D, Chanda Das SR, Kar K, Chakraborty P, Kapoor DU, et al. Nanotechnology based herbal drug delivery system: Current insights and future prospects. Curr Nanomed. 2024.
54. Mohammadi Nejad S, Özgüneş H, Başaran N. Pharmacological and Toxicological Properties of Eugenol. Turk J Pharm Sci. 2017;14(2):201-206.
55. Carvalho RPR, Ribeiro FCD, Lima TI, Ervilha LOG, de Oliveira EL, Faustino AO, et al. High doses of eugenol cause structural and functional damage to the rat liver. Life Sci. 2022;304:120696.

56. Chen J, Dong X, Zhao J, Tang G. In vivo acute toxicity of titanium dioxide nanoparticles to mice after intraperitioneal injection. J Appl Toxicol. 2009;29(4):330-337.
57. Liu H, Ma L, Zhao J, Liu J, Yan J, Ruan J, et al. Biochemical toxicity of nano-anatase TiO2 particles in mice. Biol Trace Elem Res. 2009;129(1):170-180.
58. Yousef HN, Ibraheim SS, Ramadan RA, Aboelwafa HR. The ameliorative role of eugenol against silver nanoparticles-induced hepatotoxicity in male Wistar rats. Oxid Med Cell Longev. 2022;2022(1):3820848.
59. Majeed H, Antoniou J, Fang Z. Apoptotic effects of eugenol-loaded nanoemulsions in human colon and liver cancer cell lines. Asian Pac J Cancer Prev. 2014;15(21):9159-9164.
60. Binu P, Nellikunnath Priya M, Abhilash S, Vineetha RC, Nair H. Protective effects of eugenol against hepatotoxicity induced by arsenic trioxide: An antileukemic drug. Iran J med sci. 2018;43(3):305.
61. TR DP, Haykal MN. Eugenol nanoparticle encapsulated chitosan enhances cell cycle arrest in hela human cervical cancer cells. Sys Rev Pharm. 2021;12(2).
62. Cui Y, Liu H, Ze Y, Zengli Z, Hu Y, Cheng Z, et al. Gene expression in liver injury caused by long-term exposure to titanium dioxide nanoparticles in mice. Toxicol Sci. 2012;128(1):171-185.
63. Wani MR, Maheshwari N, Shadab G. Eugenol attenuates TiO2 nanoparticles-induced oxidative damage, biochemical toxicity and DNA damage in Wistar rats: an in vivo study. nviron Sci Pollut Res Int. 2021;28(18):22664-22678.
64. Jiang Y, He P, Sheng K, Peng Y, Wu H, Qian S, et al. The protective roles of eugenol on type 1 diabetes mellitus through NRF2-mediated oxidative stress pathway. Elife. 2025;13:RP96600.
65. Su H, Wang Z, Zhou L, Liu D, Zhang N. Regulation of the Nrf2/HO-1 axis by mesenchymal stem cells-derived extracellular vesicles: implications for disease treatment. Front Cell Dev Biol. 2024;12:1397954.
66. Yuan L, Wang Y, Li N, Yang X, Sun X, Tian He, et al. Mechanism of action and therapeutic implications of Nrf2/HO-1 in inflammatory bowel disease. Antioxidants. 2024;13(8):1012.
67. Luo Y, Lu S, Dong X, Xu L, Sun G, Sun X. Dihydromyricetin protects human umbilical vein endothelial cells from injury through ERK and Akt mediated Nrf2/HO-1 signaling pathway. Apoptosis. 2017;22(8):1013-1024.
68. Alonso-Piñeiro JA, Gonzalez-Rovira A, Sánchez-Gomar I, Moreno JA, Durán-Ruiz MC. Nrf2 and heme oxygenase-1 involvement in atherosclerosis related oxidative stress. Antioxidants. 2021;10(9):1463.